ChemPubSoc Europe

DOI: 10.1002/ejoc.201900432

EurJOC European Journal of Organic Chemistry

Full Paper

Check for updates

Molecular Junctions | *Very Important Paper* | SPECIAL ISSUE

VIP

Enhanced Separation Concept (ESC): Removing the Functional Subunit from the Electrode by Molecular Design

Thomas Brandl,[a][‡] Maria El Abbassi,[b][‡] Davide Stefani,[b] Riccardo Frisenda,[b] Gero D. Harzmann,[a] Herre S. J. van der Zant,*[b] and Marcel Mayor*[a,c,d]

Dedicated to our joint friend Eugenio Coronado on the occasion of his 60th birthday

Abstract: A new concept to improve the reliability of functional single molecule junctions is presented using the *E*-field triggered switching of Fe^{II}bis-terpyridine complexes in a mechanically controlled break junction experiment as model system. The complexes comprise a push-pull ligand sensing the applied *E*-field and the resulting distortion of the Fe^{II} ligand field is expected to trigger a spin-crossover event reflected in a sudden jump of the transport current. By molecular engineering, the active centre of the complex is separated from the gold electrodes in order to eliminate undesired side-effects. Two aspects are considered to isolate the central metal ion, namely the spacing by introducing additional alkynes, and the steric shielding achieved by bulky isopropyl groups. With this small series of model complexes, a pronounced correlation is observed between the occurrence of bistable junctions and the extent of separation of the central metal ion, affirming the hypothesized *Enhanced Separation Concept* (ESC).

Introduction

Since the visionary claim of Gordon Moore[1] predicting the ongoing miniaturization of electronic circuits to improve their performance, alternative concepts to complement metal-oxide semiconductor (CMOS) technology moved into the focus of interest. Among others, single molecule devices are particularly appealing from a scientific perspective. Molecules are the smallest objects providing the structural diversity required enabling the programming of a particular electronic function into their structure. Furthermore, synthetic chemistry developed in the past centuries provides the skills required for the controlled assembly of tailor-made molecular structures.

The concept of single molecule electronics began with the hypothesized single molecule rectifier discussed theoretically by Aviram and Ratner.[2] Since then, not only the validity of their hypothesis has been demonstrated, but numerous electronic functions like transistors,[3–5] diodes,[6,7] wires,[8,9] switches[10–12] (for an overview see ref.[13]) and memory devices[14–16] (for an overview see ref.[17]) have been realized on a single-molecule level. These experimental achievements only became possible due to the parallel engagements and developments in collaborating disciplines like synthetic chemistry, experimental physics, and theory-based modelling. While single-molecule junctions based on scanning microscopy technologies often profit from the analytical power of the integration set-up providing structural insight into the spatial arrangement of the molecular structure inside the junction, this is not the case for junctions based on mechanically controlled break junctions (MCBJ) or electrode pairs prepared by electromigration. In those set-ups the transport features of the junction is in many cases the only analytical information available. The limitation in analytical diversity has been compensated by automation enabling to assemble similar junctions repeatedly collecting enough data allowing for statistical extraction of characteristic features.

Of particular interest are molecular switches as potential memory devices.[18] These junctions display at least two different conductance states, which can be switched by an external trigger. Numerous systems have been reported being addressed by various stimuli like e.g. light,[19,20] mechanical manipulation,[11,21–24] electrochemical gating,[25,26] the applied voltage,[27] or the electrical current.[28,29] We became recently interested in *E*-field triggered molecular junctions and developed a variety of model compounds sensing this parameter.

[a] *Department of Chemistry, University of Basel, St. Johanns-Ring 19, 4056 Basel, Switzerland*
E-mail: marcel.mayor@unibas.ch
https://www.chemie.unibas.ch/~mayor/
[b] *Kavli Institute of Nanoscience, Delft University of Technology, 2600 GA Delft, The Netherlands*
E-mail: H.S.J.vanderZant@tudelft.nl
http://vanderzantlab.tudelft.nl/
[c] *Karlsruhe Institute of Technology (KIT), P.O. Box 3640, 76021 Karlsruhe, Germany*
[d] *Lehn Institute of Functional Materials, School of Chemistry, Sun Yat-Sen University, Guangzhou 510275, China*
[‡] These authors contributed equally to this work.

Supporting information and ORCID(s) from the author(s) for this article are available on the WWW under https://doi.org/10.1002/ejoc.201900432.

Examples range from turnstile-type macrocycles[30] over tripodal rigid 9,9′-bisspirofluorene platforms exposing a dipole moment with a terminal coordination site[31,32] to spin cross-over complexes with geometrical arrangements defined by tailor-made ligands based on heterocycles.[33] The integration of these Fe^{II}terpyridine (tpy) derivatives exposing various functional groups in molecular junctions turned out to be challenging. Attempts based on scanning tunneling microscopy (STM) experiments suffered from the limited stability of the dicationic complex,[34] and MCBJ studies displayed a rich variety in the characteristics of the junctions pointing at numerous different arrangements of the structure between both electrodes.[33] While the extensive collection of transport data combined with the systematic variation of the molecular structure enabled to spot the correlation between junctions displaying the bistability expected for an *E*-field triggered spin cross-over and the strength of the complexes' dipole moments, the poor control over the molecules arrangement inside the junction remained unpleasant.

Here, we report our attempts to increase the control over the complexes arrangement in the single-molecule junction by improving the design of the immobilizing and electrode bridging tpy-ligand.

Results and Discussion

Molecular Design

In Figure 1 the already reported heteroleptic Fe^{II}tpy complexes **1**–**3** are displayed together with the *E*-field triggered switching concept. The tpy-ligand that all three compounds **1**–**3** have in common exposes two acetyl protected terminal thiol anchor groups. The task of this ligand is to immobilize the complex inside the junction by bridging both electrodes. The terminal thiol anchor groups are mounted in *para*-position with respect to the 4-phenylpyridine subunit of the tpy-ligand to promote current transport through the central metal ion. The second tpy-ligands of the heteroleptic complexes **1**–**3** are exposing an electron withdrawing group (EWG) on one side and an electron donating group (EDG) on the other side creating a dipole moment, which can align in an *E*-field.

The Fe^{II}tpy complexes are expected to have octahedral coordination spheres and their strong crystal fields result in a considerable splitting of the energies of the 3 orbitals with t_{2g} symmetry (d_{xy}, d_{xz}, and d_{yz}) compared to the 2 orbitals with e_g symmetry (d_{z^2} and $d_{x^2-y^2}$). The 6 coordinating electrons are thus following the *Pauli*-principle and are occupying pairwise the 3 orbitals with lower energy (d_{xy}, d_{xz}, and d_{yz}) resulting in the low-spin electron configuration (bottom of Figure 1b). By applying a voltage across the junction an *E*-field builds up distorting the octahedral coordination sphere. Distortion from the octahedral arrangement reduces the strength of the energy splitting between the orbitals with t_{2g} and e_g symmetries. The more comparable in energy they become the more *Hund*'s-rule dictates that each of the 5 orbitals must first be filled by a single electron each with parallel spin resulting in the high spin electron configuration (top of Figure 1b).[35] The spin cross-over

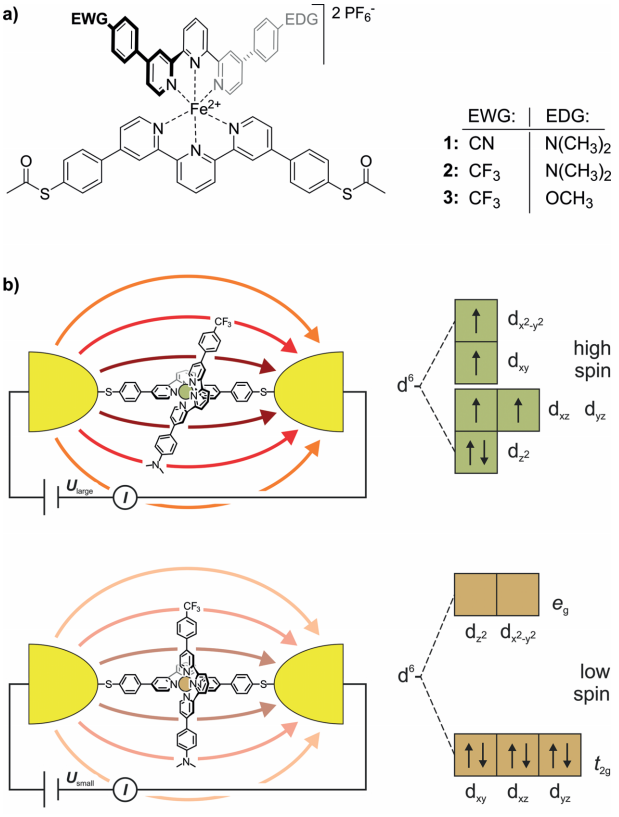

Figure 1. (a) First generation Fe^{II}terpyridine complexes **1**–**3** as model compounds for *E*-field sensitive single molecule spin cross-over switching junctions. (b) Sketch of the *E*-field triggered switching concept based on the alteration of the electronic configuration due to the distortion of the Fe^{II}tpy ligand sphere upon applying of a large enough voltage across the junction.

process should be reflected in the junctions transport current as the Fe center is integrated in the current path and its high-spin configuration is reported to be of increased electronic transparency.[36,37] The investigation of these junctions however turned out to be challenging and an increased occurrence of the expected bistability with the increased dipole moment in the series **3** to **1** was consistent with the hypothesized spin cross-over switching mechanism.[33] The still mediocre yield of functional junctions however remained incomprehensible. The working hypothesis was that the Fe-tpy complexes adopt a large variety of conformations inside the junction. In particular, the polar EWG and EDG groups exposing lone-pair comprising heteroatoms were suspected to compete with the thiol anchor groups and thereby increasing the diversity of molecular junctions.

To investigate the validity of this hypothesis, the active subunit exposing functional groups (EWG and EDG) competing with the intended anchor groups should be moved further away from the electrode surfaces. As sketched in Figure 2a, two molecular design parameters addressing this task have been identified: 1) the *distance* of the "active subunit" and the electrode surface and 2) the bulkiness of substituents sterically separating the "active subunit" from the electrode (*bulky shield* in Figure 2a). For simplicity, we named the approach "Enhanced Separation Concept" (ESC).

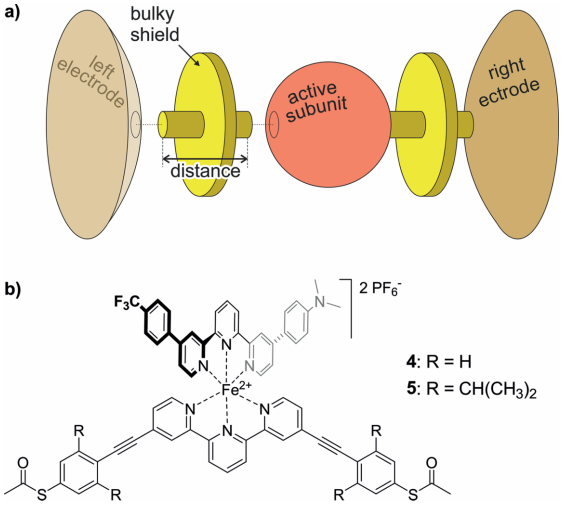

Figure 2. (a) The "Enhanced Separation Concept" (ESC) removing the functional subunit from the electrode surface by increasing the distance and/or by introducing sterically shielding substituents. (b) Heteroleptic Fe^{II} model complexes **4** and **5** to investigate the ESC.

To verify the ESC, the heteroleptic Fe^{II} model complexes **4** and **5** were considered as optimized derivatives of the parent compound **2** (Figure 2b). While **4** enhances the distance between electrode and Fe-center by introducing an additional alkyne group, derivative **5** further enhances the steric shielding by additional isopropyl groups in *meta*-positions with respect to the thiol anchor groups.

Synthesis

The series of tpy-ligands of the 1st generation have been assembled by engaging the dichloro-tpy precursor **9** into a *Suzuki* cross-coupling reaction.[33,38] To introduce an additional alkyne unit, a cross-coupling protocol for the also Pd-catalyzed *Sonogashira* reaction was optimized. The assembly of both target complexes is displayed in Scheme 1.

For the assembly of **4**, the terpyridine compound **11** was required. Starting with commercial 4-bromobenzenethiol **6**, the thiophenol was first protected by treating **6** in an excess of trimethyl(vinyl)silane with di-*tert*-butyl peroxide (DTBP) as radical initiator. With this variation of a reported procedure,[39] the TMS-ethyl protected thiophenol **7** was obtained in 98 % yield as colorless oil. In a *Sonogashira* coupling reaction, the alkyne synthon was introduced by substituting the bromine of **7** with a trimethylsilyl (TMS)-masked acetylene. The crude reaction product was liberated from its alkyne protection group by treatment with K_2CO_3 in a mixture of methanol (MeOH) and tetrahydrofuran (THF). This adapted procedure[40] provided the alkyne **8** in 55 % yield after column chromatography (CC). 4,4′′-Dichloro-2,2′:6′,2′′-terpyridine **9** was synthesized according to our already reported procedure,[38] and its chlorine atoms were substituted by the alkyne **8** in a variation of the *Sonogashira* cross-coupling reaction which does not require the addition of copper salts. The latter being an interesting aspect reducing the frequently observed competing copper catalyzed oxidative acetylene coupling. The catalytic system was assembled in-situ

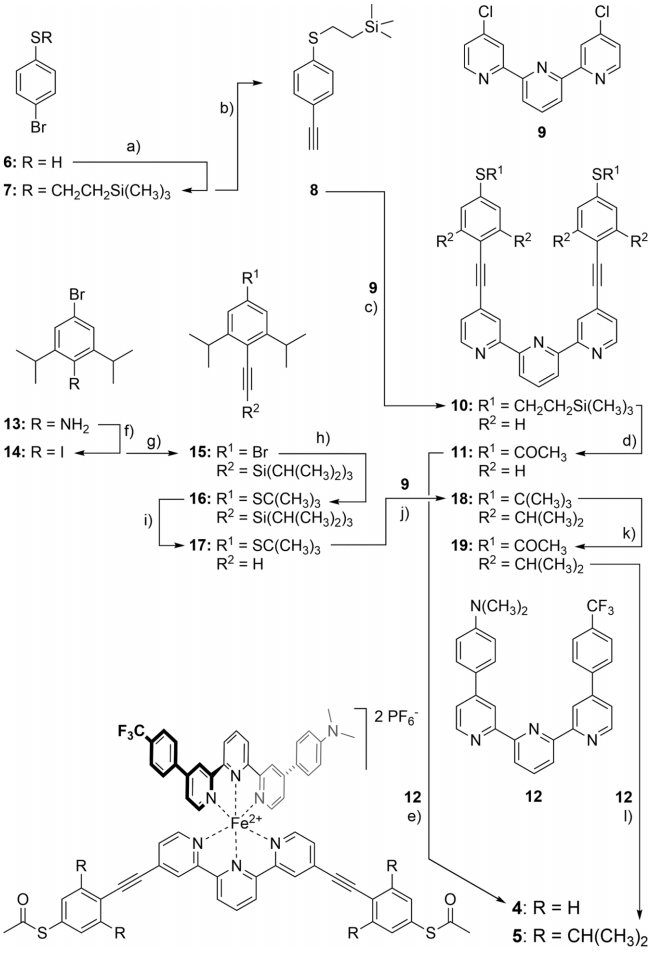

Scheme 1. Synthesis of the Fe^{II}tpy complexes **4** and **5**. Reagents and conditions: (a) $CH_2CHSi(CH_3)_3$, DTBP, microwave (MW), 100 °C, 5.5 h, 98 %; (b) 1.) $HCCSi(CH_3)_3$, $Pd(PPh_3)_2Cl_2$, CuI, $HNEt_2$, 60 °C, 18 h; 2.) K_2CO_3, MeOH/THF (1:1), r.t., 1 h, 55 %; (c) Cs_2CO_3, $Pd(MeCN)_2Cl_2$, X-Phos, propionitrile, reflux, 3.5 h, 93 %; (d) 1.) TBAF, THF, r.t., 1.5 h, 2.) AcCl, −10 °C, 2 h, 95 %; (e) 1.) $FeCl_2$, MeOH/DCM/H_2O (1:1:5), r.t., 1 h; 2.) NH_4PF_6, 19 %; (f) 1.) $NaNO_2$, H_2SO_4/H_2O/MeCN, 0 °C, 2.) KI, H_2O, r.t., 1 h, 89 %; (g) (triisopropylsilyl)acetylene, $Pd(dppf)Cl_2$, CuI, DIPA/toluene (1:3), 80 °C, 14 d, 54 %; (h) 2-methyl-2-propane-thiol, 1,4-bis(diphenylphosphino)butane, K_2CO_3, $Pd(OAc)_2$, 1-methyl-2-pyrrolidone, 100 °C, 24 h, 39 %; (i) TBAF, DCM, 10 min, quant.; (j) Cs_2CO_3, $Pd(MeCN)_2Cl_2$, X-Phos, propionitrile, reflux, 16 h, 65 %; (k) $Bi(OTf)_3$, AcCl, MeCN/toluene (1:1), r.t., 1 h, 92 %; (l) 1.) $FeCl_2$, DCM/MeOH (1:1), r.t., 1 h, 2.) H_2O, NH_4PF_6, 45 %.

by adaptation of a reported protocol[41] using $Pd(MeCN)_2Cl_2$ as palladium source and 2-dicyclohexylphosphino-2′,4′,6′-triisopropylbiphenyl (X-Phos) as ligand in propionitrile with Cs_2CO_3 as base. The reaction was refluxed and monitored by thin layer chromatography (TLC). Work up after 3.5 hours provided the tpy-ligand **10** in very good 93 % yield after CC. Transprotection with tetrabutylammonium fluoride (TBAF) and acetyl chloride (AcCl) in THF provided the desired tpy-ligand **11** in very good 95 % isolated yield. The push-pull tpy-ligand **12** was assembled following our already reported procedure.[33] With both ligands **11** and **12** in hands, the heteroleptic complex **4** was synthesized using a simple but effective statistical strategy. Thus, both ligands were suspended together with $FeCl_2$ in a mixture of dichloromethane (DCM), MeOH, and water (H_2O). The complexes were precipitated by addition of an excess of ammoni-

umhexafluorophosphate (NH_4PF_6) and the desired heteroleptic complex was separated from the homoleptic ones by preparative reversed-phase HPLC giving the desired $Fe^{II}tpy_2$ derivative **4** as dark purple solid in 19 % isolated yield.

The assembly of the second complex **5** was expected to be more challenging due to the bulky isopropyl groups, which might also interfere with the intended coupling steps. However, a very comparable strategy was applied. The required alkyne **17** was assembled in 4 steps from the commercially available 4-bromo-2,6-diisopropylaniline **13**. The order of functional group transformations on this building block turned out to be crucial as initial attempts first introducing the masked thiol substituent reduces the reactivity of the halide in *para*-position for the subsequent coupling reaction to a level making the further development of the building block impossible. Thus, the alkyne-synthon was introduced first. The amine was transformed into an iodine in a *Sandmeyer* reaction following a classical protocol: Treatment of **13** with sodium nitrite in a mixture of sulfuric acid, H_2O, and acetonitrile (MeCN) at 0 °C provided the diazonium salt, which was subsequently converted into the iodine **14** by quenching with potassium iodide. Work-up followed by CC provided **14** as light brown solid in 89 % isolated yield. To introduce the alkyne-synthon, we hoped that the increased reactivity of the iodine substituent in Pd-catalyzed coupling conditions would outperform the competing sterically less buried bromine in **14**. To further increase the potential steric issues, we were forced to use the triisopropylsilyl (TIPS) masked acetylene as the more compact TMS-masking group used above is not surviving the rather harsh reaction conditions required for the introduction of the *tert*-butyl masked thiol substituent. To our delight we found optimized *Sonogashira* conditions mainly addressing the iodine even though elevated temperatures were required and the substitution was slow. Using $Pd(dppf)Cl_2$ and CuI as catalytic system in an argon saturated mixture of diisopropylamine (DIPA) and toluene at 80 °C the arylalkyne **15** was slowly formed from the iodoaryl **14** and the TIPS-acetylene. The course of the reaction was monitored by gas-chromatography (GC) and the disappearance of TIPS-acetylene was compensated by the addition of additional equivalents. After 2 weeks the reaction was worked up in spite of remaining iodoaryl **14** and the desired arylalkyne **15** was isolated in 54 % yield after CC. Also the substitution of the bromine in **15** with *tert*-butylmercaptane was enabled by Pd-catalyzation. The aryl bromide **15** and *tert*-butylmercaptane were dissolved in 1-methyl-2-pyrrolidone with $Pd(OAc)_2$ as Pd-source and 1,4-bis(diphenylphosphino)butane as ligand of the catalyst and K_2CO_3 as base. After 24 h at 100 °C the building block **16** was isolated in poor 39 % isolated yield after CC. The alkyne **17** was liberated quantitatively by treatment with TBAF in DCM at room temperature. For the twofold cross-coupling between the alkyne **17** and the dichloro-tpy **9** the same reaction conditions as for the sterically less demanding alkyne **8** in the assembly of **10** have been applied. Thus **9** and 2.5 equivalents of **17** were exposed to the catalyst assembled from $Pd(MeCN)_2Cl_2$ and X-Phos in situ and the base Cs_2CO_3 in refluxing propionitrile for 16 h. In spite of the elongated reaction time compared with the assembly of **10**, the tpy-ligand exposing *tert*-butyl masked thiols **18** was isolated in only 65 % yield by CC reflecting the sterically more demanding situation in this case. The transprotection from the *tert*-butyl groups in **18** to the acetyl groups in **19** was achieved almost quantitatively by treatment with bismuth(III) trifluoromethanesulfonate and AcCl in MeCN/toluene at room temperature. The $Fe^{II}tpy_2$ target compound **5** was obtained by a similar protocol as applied above for the assembly of **4**. Equimolar amounts of both ligands **12** and **19** were stirred for 1 h together with $FeCl_2$ in a DCM/MeOH mixture. The crude was transferred to an aqueous solution and the $Fe^{II}tpy_2$ complexes were precipitated by NH_4PF_6. The heteroleptic target complex **5** was isolated by preparative reversed-phase HPLC as dark purple solid in 45 % yield.

The identity of the $Fe^{II}tpy_2$ target complexes was fully corroborated by their analytical data. For their transport analyses in a mechanically controlled break junction (MCBJ) fresh solutions were prepared as the dissolved heteroleptic complexes **4** and **5** are in an equilibrium slowly forming both homoleptic complexes. Stability experiments were performed with complex **1** and a half-life time ($t_{1/2}$ = 24 h) exceeding substantially the duration of the deposition procedure (5 minutes) was determined.[33] While comparable stability behaviors were observed for the heteroleptic complexes **2** and **4**, the stability investigations of **5** revealed its considerably increased stability probably arising from the steric shielding of the metal ion. According to preliminary kinetic studies (see supporting information), the complex **5** decomposes in acetonitrile at 25 °C with a half-life time of about $t_{1/2}$ = 316 h. Thereby, the heteroleptic complex not only forms an equilibrium with its homoleptic relatives, but slowly decomposes irreversibly into another yet unknown compound.

The target structures and their precursors and intermediates on the synthetic path have been characterized by ^1H- and ^{13}C-NMR spectroscopy and mass spectrometry.

Transport Experiments

Similarly to our previous study on complex **2**,[33] single-molecule-transport measurements of compound **4** and **5** were performed in a MCBJ in vacuo at liquid helium temperature in the case of complex **4** and at liquid nitrogen temperature for complex **5**. A schematic of the experiment is shown in Figure 3. The sample consists of a lithographically patterned gold wire suspended onto a flexible substrate coated with a polyimide film, which can be bent to stretch the gold wire. When the wire ruptures, two atomically sharp electrodes are formed and the distance between them can be tuned with sub-nanometer precision.

In analogy to our already reported transport studies with complex **2**,[33] the MCBJ sample was decorated with the complex under investigation prior to the breaking and measuring sequence. A freshly prepared solution of either **4** or **5** (0.5 mM in acetonitrile) was deposited on the MCBJ sample and the solvent was evaporated. The measurement chamber was evacuated to 10^{-7} mbar and cooled down. At low temperature, the gold wire was repeatedly broken and fused in the presence of molecules hundreds of times and current-voltage characteristics were recorded during every breaking cycle.

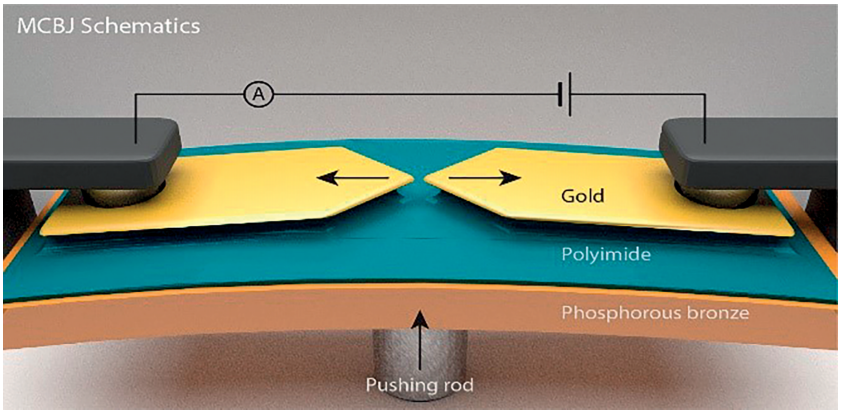

Figure 3. Sketch of the MCBJ set-up enabling the repetitive formation of single molecule junctions.

The breaking traces were first divided into two main categories, namely the ones forming a molecular junction and the empty ones. While the first category displays current plateaus indicative of molecules bridging the gap between the electrodes, the empty junctions show an exponential decrease of the current with the displacement. The left pie chart of Figure 5 shows the fraction (blue segment) forming a molecular junction for each complex **2**, **4** and **5**.

At low temperature the molecular junctions are stable enough to record the *IV* characteristic. Based on the analysis of the *IV* behaviors the molecular junctions were further divided into the ones displaying bistability features (orange segment in the right pie charts of Figure 5) and the ones without. A spin crossover event in the central metal complex is expected to result in an immediate variation of the transport current, which is displayed by bistability features in the recorded *IV*. In Figure 4, typical examples of the distinguished categories are displayed for the investigation of complex **5**. A smooth increase of the current with the applied voltage (Figure 4a) represent molecular junctions without voltage-triggered switching events in the investigated voltage window. Junctions with bistable *IV* traces due to switching events displayed either negative differential conductance (NDC) features (Figure 4b) or sudden jumps to higher conductance values (Figure 4c). The NDC depression at about –0.25 V is clearly visible in Figure 4b, while the representative example in Figure 4c displays current jumps at both, negative and positive bias at values of around –0.5 V and 0.7 V, respectively.

The variety of the *IV* traces from different switching molecular junctions most likely reflects the diversity of both the spatial arrangements of the complex inside the junction and the atomistic realization of the electrodes' surfaces/shapes. 542, 1315 and 653 breaking cycles were measured in the case of complex **2**, **4** and **5**, respectively. Figure 5 shows the proportion of breaking events presenting a molecular signature. Compared to the 7 % already recorded for **2**,[33] the ratio of molecular junctions increased to 37 % and 21 % with the new complexes **4** and **5**. While it is tempting to correlate the increased likeliness of molecular junction formation with the expanded structure of their terpyridine ligand comprising acetylene spacers, the data set with only two additional complexes is too small for reliable conclusions. In an earlier study we recorded for five different complexes of the dimension of **2**, molecular junction formation probabilities between 6 % and 25 %[33] documenting the large and to some extent random dispersion of the ratios of molecular junctions. However, in spite of the small experimental data set, the trend of larger ratios of molecular junctions with the two complexes with an immobilizing tpy-ligand enlarged by ethynyl subunits (**4** and **5**) supports the molecular design hypothesis that more exposed anchor groups facilitate the immobilization of the compound between both electrodes.

Even more impressive is the substantial increase in molecular junctions displaying bistability within the series **2**, **4**, and **5** (orange segment in Figure 6). The ratio of junctions with bistable *IV*s increases from 43 % for **2**, over 56 % for **4**, to climax in 98 % for **5**. Both molecular design optimizations (the increasing of

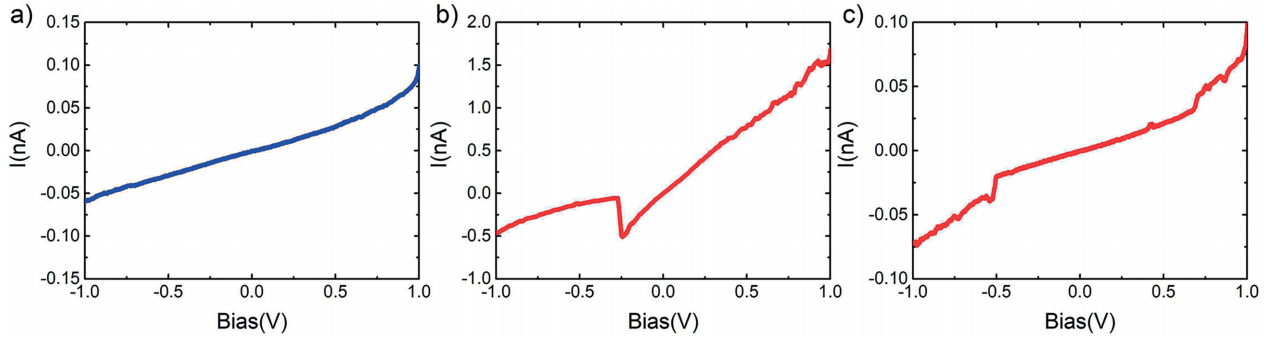

Figure 4. Various types of *IV*s observed for molecular junctions of complex **5**. (a) *IV*-behavior without bistability features; (b) *IV* with a NDC jump at –0.25 V; (c) *IV* with current jumps at both, negative and positive voltages.

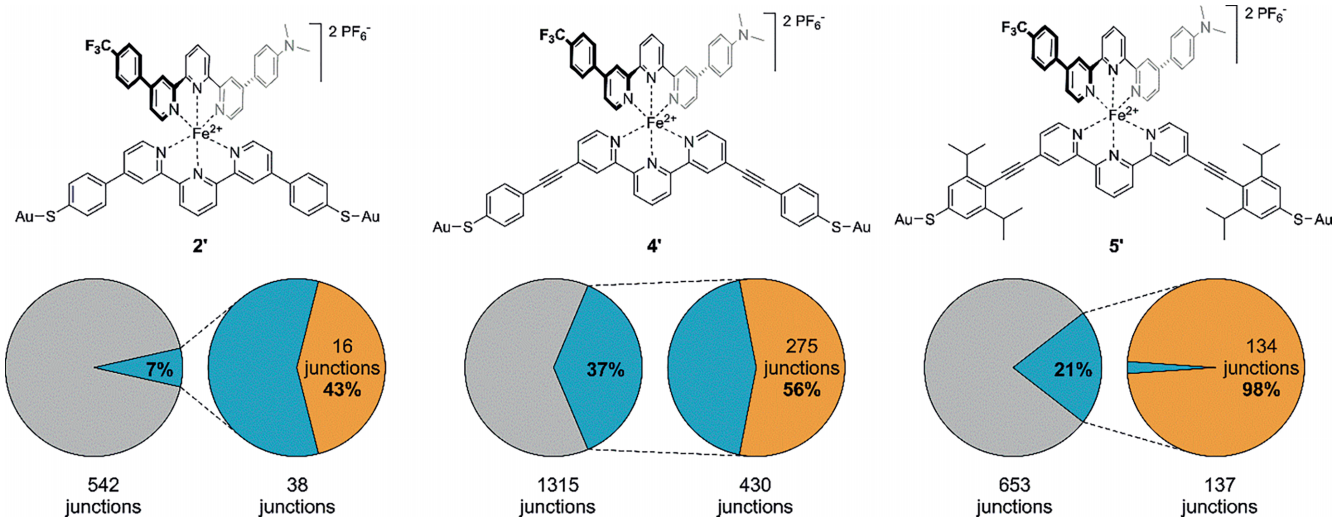

Figure 5. Statistical analysis of the MCBJ experiments. Top: Sketch of the immobilized complexes **2′**, **4′** and **5′**. Bottom: The left pie chart displays the fractions of molecular junctions formed (blue segment). The right pie chart shows the fraction of molecular junctions with bistability features (orange segment).

the spacing between electrode and central complex and the enlarged shielding of the complex by bulky substituents) are improving the formation of junctions comprising a functional complex. The substantial improvement by the introduction of isopropyl groups in **5** probably is a combination of several aspects. Their bulkiness results in a better defined immobilization of the complexes via the S-anchor groups and disfavors contacts between the phenyl-π-system of the immobilizing tpy-ligand and the electrode surface. Furthermore, their bulkiness leads to a better organization of the entire complex by filling up the empty space in-between both ligands. Thus, the more densely packed complex **5** offers less interaction surface for π-gold interactions,[42] which are likely to be mainly responsible for molecular junctions without switching events. The fixation of the push-pull tpy-ligand by such interactions prevents any alteration of the coordination sphere and thus also the intended switching.

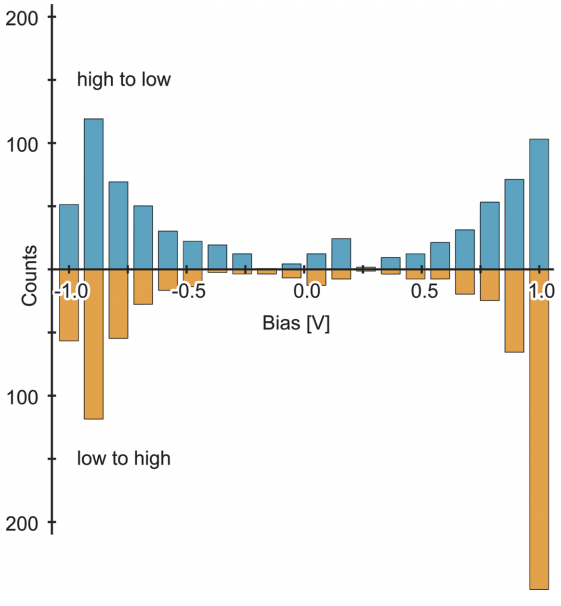

Figure 6. Statistics of the switching bias voltage for junctions with compound **5′**.

Further details concerning the nature of the molecular switching was collected for the junctions with **5** by analyzing the statistics of the bias voltage at which the switching between two conductance states occurs. As displayed in Figure 6, the switching occurs more often at higher bias voltage values with a maximum around –0.9 V in the negative region. The symmetrical distribution of the events mirrored at about zero bias was expected for switching events depending exclusively on the magnitude of the electric field and not on its polarity.

The bias voltage required to initiate the switching is of hundreds of meV, which is much larger than the thermal energy at 77 K (≈ 6 meV) or even at room temperature (25 meV). Therefore, we expect that thermal effects do not play an important role in triggering the bistability of the molecule. On the other hand, junction stability is usually affected by the higher temperature, yet the higher stability of the junctions comprising **5** allowed their investigation at ≈ 77 K.

Conclusions

A new molecular design approach named "*Enhanced Separation Concept*" (ESC) to improve the reliability of functional molecules in single molecule junctions is presented. This revolves around the principle of reducing the interaction between the electrode and active subunit. This is achieved by increasing the separation between active subunit and the electrode surface (**4**, **5**) and the addition of bulky substituents to shield the active subunit (**5**). The ESC was benchmarked on the two model complexes **4** and **5**, which both comprise the same push-pull Fe^{II}tpy ligand that can be distorted under electric field by triggering a spin-crossover transition. The occurrence of bistable single molecule junctions is analyzed by integrating the complexes in MCBJ experiments at low temperature. A substantial increase of bistable junctions is observed by separating the functional $Fe^{II}(tpy)_2$ center in the series **2**, **4**, and **5** with 43, 56 and 98 %, respec-

tively. The findings not only corroborate the hypothesized "*Enhanced Separation Concept*", but also demonstrate the optimization power of molecular design.

Motivated by these results we are currently developing the complexes further with foci on both, their chemical stability and their spatial arrangement inside the junction.

Experimental Section

General Procedures: All commercial available chemicals were used without further purification. Dry solvents were used as crown cap and purchased from Acros Organics and Sigma-Aldrich. NMR solvents were obtained from CIL Cambridge Isotope Laboratories, Inc. (Andover, MA, USA) or Sigma-Aldrich. All NMR experiments were performed on Bruker Avance III or III HD, two or four-channel NMR spectrometer operating at 400.13, 500.13 or 600.27 MHz proton frequency. The instruments were equipped with direct observe BBFO, indirect BBI or cryogenic four-channel QCI (H/C/N/F) 5 mm probes all with self-shielded *z*-gradient. The experiments were performed at 298K or 295K. All chemical shifts (δ) are reported in parts per million (ppm) relative to the used solvent and coupling constants, (*J*) are given in Hertz (Hz). The multiplicities are written as: s = singlet, d = doublet, t = triplet, hept = heptet, dd = doublet of doublet, m = multiplet. Gas Chromatography (GC–MS) was performed on a Shimadzu GC–MS-QP2010 SE gas chromatograph system, with a ZB-5HT inferno column (30 m × 0.25 mm × 0.25 mm), at 1 mL/min He-flow rate (split = 20:1) with a Shimadzu mass detector (EI 70 eV). Flash column chromatography (FCC) was performed with SiliaFlash® P60 from SILICYCLE with a particle size of 40–63 µm (230–400 mesh) and for TLC Silica gel 60 F_{254} glass plates with a thickness of 0.25 mm from Merck were used. The detection was observed with a UV-lamp at 254 or 366 nm. Gel Permeation Chromatography (GPC) was performed on a Shimadzu Prominence System with PSS SDV preparative columns from PSS (2 columns in series: 600 mm × 20.0 mm, 5 µm particles, linear porosity "S", operating ranges: 100–100.000 g mol^{-1}) using chloroform as solvent. For HPLC a Shimadzu LC-20AD and a LC-20AT HPLC was used equipped with a diode array UV/Vis detector (SPD-M10A VP from Shimadzu, λ = 200–600 nm) and a column oven Shimadzu CTO-20AC for analytical measurements. The used column was a Reprosil 100 C18, 5 µm, 250 × 16 mm; Dr. Maisch GmbH. For preparative HPLC a Shimadzu LC-20Ap and a LC-20Ap was used equipped with a diode array UV/Vis detector (SPD-20A from Shimadzu, λ = 200–600 nm). The used column was a Reprosil 100 C18, 10 µm,250 × 30 mm; Dr. Maisch GmbH. High-resolution mass spectra (HRMS) were measured as HR-ESI-ToF-MS with a Maxis 4G instrument from Bruker or as HR-EI-MS spectrometry with a DFS double-focusing (BE geometry) magnetic sector mass spectrometer (ThermoFisher Scientific, Bremen, Germany). Mass spectra were measured with electron ionization (EI) at 70 eV, solid probe inlet, a source temperature of 200 °C, an acceleration voltage of 5 kV, and a resolution of 10'000. The instrument was scanned between e.g. *m/z* 300 und 350 at scan rate of 100- 200 s/decade in the electric scan mode. Perfluorokerosene (PFK, Fluorochem, Derbyshire, UK) served for calibration.

2-[(4-Bromophenyl)thio]ethyltrimethylsilane (7): Compound **7** was prepared according to reported literature protocols.[40,41,43] A microwave vessel was charged with 4-bromothiophenol (**6**, 11.1 g, 58.8 mmol, 1.00 equiv.), vinyltrimethylsilane (7.29 g, 10.7 mL, 70.6 mmol, 1.20 equiv.) and di-*tert*-butyl peroxide (1.29 g, 1.61 mL, 8.82 mmol, 0.15 equiv.). The reaction mixture was degassed before the vessel was closed and heated to 100 °C for 5.5 h. After cooling down to room temperature the reaction mixture was diluted with *n*-hexane and washed twice with aqueous NaOH solution (1 M, 50 mL). The combined aqueous phases were extracted with *n*-hexane (3 × 50 mL) and the combined organic layers were dried over $MgSO_4$, filtered and subsequently concentrated under reduced pressure. Finally the crude product was purified by vacuum distillation (b.p.: 103 °C at 9.4 × 10^{-2} mbar) to yield the desired product **7** as a colorless liquid in a yield of 98 % (16.7 g, 57.8 mmol).

Analytical Data for 7: ^{1}H-NMR (400 MHz, $CDCl_3$, 22 °C): δ = 7.37 (d, *J* = 8.6 Hz, 2H), 7.14 (d, *J* = 8.6 Hz, 2H), 2.91 (m, 2H), 0.90 (m, 2H), 0.02 (s, 9H). ^{13}C-NMR (101 MHz, $CDCl_3$, 22 °C): δ = 136.68, 132.02, 130.63, 119.59, 29.88, 16.97, –1.56. MS (EI^+, 70 eV): *m/z* [ion, intensity (%)] = 290.0 (M^+, 8), 73.0 (TMS^+, 100). EA: Anal. calcd. for $C_{11}H_{17}BrSSi$ (MW: 289.31): C, 45.67; H, 5.92; N, 0.00; found C, 45.70; H, 5.95; N, 0.00.

{2-[(4-Ethynylphenyl)thio]ethyl}trimethylsilane (8): Compound **8** was prepared in two steps by adapting a previously reported literature procedure.[40] 2-[(4-Bromophenyl)thio]ethyltrimethylsilane (**7**, 810 mg, 2.80 mmol, 1.00 equiv.), TMS-acetylene (58.9 mg, 310 µmol, 0.11 equiv.), $Pd(PPh_3)_2Cl_2$ (199 mg, 280 µmol, 10 mol-%) and CuI (810 mg, 2.80 mmol, 1.00 equiv.) were charged into a Schlenk tube, dissolved in diethylamine (50 mL) and degassed for 30 min before the reaction vessel was sealed and heated to 60 °C for 18 h. Subsequently the reaction was cooled down to room temperature before being quenched by the addition of water and dilution with DCM. Saturated NH_4Cl solution (30 mL) and brine were added prior to repeated extraction of the mixture with DCM (4 × 30 mL). The combined organic layers were dried with $MgSO_4$, filtered and concentrated under reduced pressure to yield the crude product which was now purified by FCC using a gradient of solvents reaching from pure *n*-hexane to a mixture of *n*-hexane/EtOAc (17:3). The column yielded 821.4 mg of a mixture of starting material and TMS protected **8**. In the second step 767 mg (at least 2.5 mmol) of the described mixture were charged into a round-bottomed flask and K_2CO_3 (873 mg, 6.25 mmol) was added. The reagents were dissolved in a 1:1 mixture of MeOH and THF (15 mL each) and the mixture was stirred for 1 h at room temperature, until the deprotection was finished (monitored by TLC). After DCM and brine were added to the reaction mixture the same was extracted with DCM (4 × 30 mL). The combined organic layers were dried over $MgSO_4$ and concentrated to yield the crude product which was now purified by FCC using a gradient of solvents reaching from pure *n*-hexane to a mixture of *n*-hexane/DCM (9:1). Thus the desired product {2-[(4-ethynylphenyl)thio]ethyl}trimethylsilane (**8**) was obtained quantitatively (338 mg, 1.44 mmol) from this reaction step. Apart from this the original starting material was reisolated (283 mg, 0.98 mmol). Therefore, the desired target compound **8** was isolated in an overall yield of 55 % (362 mg, 1.54 mmol), whereas the starting material was recovered in a yield of 37 % (303 mg, 1.05 mmol). The spectroscopic data for this compound was identical to those reported in literature.[40]

4,4′′-Bis[(4-{[2-(trimethylsilyl)ethyl]thio}phenyl)ethynyl]-2,2′:6′,2′′-terpyridine (10): 10 was prepared by adapting a literature reported protocol.[41] 4,4′′-dichloro-2,2′:6′2′′-terpyridine (**9**, 60.4 mg, 200 µmol, 1.00 equiv.), {2-[(4-ethynylphenyl)thio]ethyl}trimethylsilane (**8**) (1.57 mg, 600 µmol, 3.00 equiv.), the base Cs_2CO_3 (393 mg, 1.20 mmol, 6.00 equiv.), the pre-catalyst $Pd(MeCN)_2Cl_2$ (35.4 mg, 6.00 µmol, 3 mol-%) and the ligand 2-dicyclohexylphosphino-2′,4′,6′-triisopropylbiphenyl (X-Phos) (8.85 mg, 18.0 µmol, 9 mol-%) were charged into a two-necked flask with reflux condenser and suspended in previously degassed propionitrile (10 mL). The reaction mixture was heated to reflux for 3.5 h until the reaction was finished according to TLC. Prior to workup the reaction mixture was

cooled down to room temperature and successively diluted with DCM and saturated NH_4Cl solution. Now the reaction mixture was extracted with DCM (5 × 30 mL) before the combined organic phases were dried over $MgSO_4$, filtered and concentrated under reduced pressure. Finally the crude product was further purified by FCC using EtOAc/*n*-hexane (3:17) as eluent to yield the disubstituted product 4,4′′-bis[(4-{[2-(trimethylsilyl)ethyl]thio}phenyl)-ethynyl]-2,2′:6′,2′′-terpyridine **10** as a brown sticky solid in a yield of 93 % (129 mg, 185 µmol).

Analytical Data for 10: ^{1}H-NMR (500 MHz, $CDCl_3$, ppm, 25 °C): δ = 8.70 (dd, *J* = 1.6, 0.8 Hz, 2H), 8.68 (dd, *J* = 5.0, 0.6 Hz, 2H), 8.46 (d, *J* = 7.8 Hz, 2H), 7.98 (t, *J* = 7.8 Hz, 1H), 7.51 (d, *J* = 8.5 Hz, 4H), 7.42 (dd, *J* = 5.0, 1.6 Hz, 2H), 7.25 (d, *J* = 8.3 Hz, 4H), 3.01 (m, 4H), 0.96 (m, 4H), 0.06 (s, 18H). ^{13}C-NMR (126 MHz, $CDCl_3$, ppm, 25 °C): δ = 156.45, 155.18, 149.27, 140.07, 138.10, 132.52, 132.35, 127.59, 121.58, 123.24, 121.61, 118.85, 94.09, 87.67, 28.78, 16.66, −1.59. HRMS (ESI-ToF): *m/z* calcd. for $[C_{41}H_{43}N_3S_2Si_2 + H]^+$: 698.2510, found 698.2501.

S,S′-{[(2,2′:6′,2′′-terpyridine)-4,4′′-diylbis(ethyne-2,1-diyl)]bis-(4,1-phenylene)} diethanethioate (11): The acetyl-protected thiol **11** was prepared by the transprotection of the ethyl-TMS protected 4,4′′-bis[(4-{[2-(trimethylsilyl)ethyl]thio}phenyl)ethynyl]-2,2′:6′,2′′-terpyridine (**10**). An oven-dried round-bottom flask was charged with terpyridine precursor (**10**, 76.8 mg, 110 µmol, 1.00 equiv.) and put under inert atmosphere. Subsequently **10** was dissolved in rigorously degassed THF (20 mL) as the solvent, before TBAF (1 M in THF, 1.10 mL, 1.10 mmol, 10.0 equiv.) was added which caused the former colourless solution to turn orange-red immediately. After 1.5 h of stirring the reaction mixture was cooled down to −10 °C prior to the dropwise addition of previously degassed acetyl chloride (1.74 g, 1.59 mL, 22.0 mmol, 200 equiv.) to the red solution which subsequently turned colourless again followed by a bright yellow colour. After further 2 h in the cooling bath the reaction was cautiously quenched by the addition of saturated $NaHCO_3$ solution. The reaction mixture was extracted with DCM (4 × 40 mL), before the combined organic phases were dried over $MgSO_4$, filtered and concentrated under reduced pressure. Finally the resulting crude product was further purified by FCC using a solvent gradient ranging from EtOAc/*n*-hexane (1:3) via EtOAc/*n*-hexane (1:1) up to pure EtOAc to yield the desired disubstituted product S,S′-{[(2,2′:6′,2′′-terpyridine)-4,4′′-diylbis(ethyne-2,1-diyl)]bis(4,1-phenylene)} diethanethioate (**11**) in an excellent yield of 95 % as a brownish solid (60.5 mg, 104 µmol).

Analytical Data for 11: ^{1}H-NMR (400 MHz, $CDCl_3$, ppm, 22 °C): δ = 8.72 (dd, *J* = 1.6, 0.9 Hz, 2H), 8.71 (dd, *J* = 5.0, 0.7 Hz, 2H), 8.48 (d, *J* = 7.8 Hz, 2H), 7.99 (t, *J* = 7.8 Hz, 1H), 7.64 (d, *J* = 8.4 Hz, 4H), 7.44 (dd, *J* = 4.9, 1.6 Hz, 2H), 7.43 (d, *J* = 8.4 Hz, 4H), 2.45 (s, 6H). ^{13}C-NMR (101 MHz, $CDCl_3$, ppm, 22 °C): δ = 193.27, 156.53, 155.13, 149.36, 138.17, 134.47, 132.62, 132.13, 129.41, 125.68, 123.54, 123.35, 121.69, 93.19, 88.90, 30.49. HRMS (ESI-ToF): *m/z* calcd. for $[C_{35}H_{23}N_3O_2S_2 + H]^+$: 582.1304, found 582.1302.

{[Fe(11)(12)]$^{2+}$[(PF$_6$)$^-$]$_2$} (4): In this case a statistic reaction had to be performed in which an equimolar amount of the terpyridine precursors was used. Thus S,S′-{[(2,2′:6′,2′′-terpyridine)-4,4′′-diylbis(ethyne-2,1-diyl)]bis(4,1-phenylene)} diethanethioate (**11**, 29.1 mg, 50.0 µmol, 1.00 equiv.) and *N*,*N*-dimethyl-4-{4′′-[4-(trifluoromethyl)phenyl]-(2,2′:6′,2′′-terpyridin)-4-yl}aniline (**12**, 24.8 mg, 50.0 µmol, 1.00 equiv.) were mixed with $FeCl_2$ (6.34 mg, 50.0 µmol, 1.00 equiv.). The reagents were suspended in MeOH (20 mL), DCM (20 mL), and water (100 mL). The reaction mixture was stirred for 1 h and then, for the anion exchange, NH_4PF_6 (407 mg, 2.50 mmol, 50.0 equiv.) was used. The complex precipitated, was filtered and washed several times with H_2O. As expected the crude product turned out to be a statistical mixture of the two homoleptic complexes and the heteroleptic complex. To obtain the desired heteroleptic target complex **4** the crude mixture was subjected to purification by preparative reversed-phase HPLC using a solvent gradient ranging from H_2O/MeCN (50:50) up to H_2O/MeCN (5:95) at a flow rate of 20 mL/min yielding the product **4** as a dark purple solid in a yield of 19 % (13.2 mg, 9.00 µmol).

Analytical Data for 4: ^{1}H-NMR (400 MHz, CD_3CN, ppm, 22 °C): δ = 9.07 (d, $^3J_{H,H}$ = 8.1 Hz, 2H, $H3_{(asym)}'/H5_{(asym)}'$), 8.95 (d, $^3J_{H,H}$ = 8.1 Hz, 2H, $H3_{(sym)}'/H5_{(sym)}'$), 8.78 (d, $^4J_{H,H}$ = 1.6 Hz, 1H, $H3_{(asym)}*/H3_{(asym)}''*$), 8.75 (t, $^3J_{H,H}$ = 7.7 Hz, 1H, $H4_{(sym)}'$), 8.73 (t, $^3J_{H,H}$ = 7.8 Hz, 1H, $H4_{(asym)}'$), 8.69 (d, $^4J_{H,H}$ = 1.9 Hz, 1H, $H3_{(asym)}*/H3_{(asym)}''*$), 8.62 (d, $^4J_{H,H}$ = 1.1 Hz, 2H, $H3_{(sym)}/H3_{(sym)}''$), 7.90 (d, $^3J_{H,H}$ = 8.4 Hz, 2H, $H_{phenyl(push)}$), 7.84 (d, $^3J_{H,H}$ = 8.5 Hz, 2H, $H_{phenyl(push)}$), 7.69 (d, $^3J_{H,H}$ = 9.1 Hz, 2H, $H_{phenyl(pull)}$), 7.60 (d, $^3J_{H,H}$ = 8.5 Hz, 4H, $H_{phenyl(sym)}$), 7.48 (d, $^3J_{H,H}$ = 8.5 Hz, 4H, $H_{phenyl(sym)}$), 7.37 (dd, $^3J_{H,H}$ = 6.0 Hz, $^4J_{H,H}$ = 2.0 Hz, 1H, $H5_{(asym)}*/H5_{(asym)}''*$), 7.28 (dd, $^3J_{H,H}$ = 6.1 Hz, $^4J_{H,H}$ = 2.0 Hz, 1H, $H5_{(asym)}*/H5_{(asym)}''*$), 7.17 (dd, $^3J_{H,H}$ = 5.9 Hz, $^4J_{H,H}$ = 1.7 Hz, 2H, $H5_{(sym)}/H5_{(sym)}''$), 7.12 (app. d, $^3J_{H,H}$ = 6.0 Hz, 3H, $H6_{(sym)}/H6_{(sym)}''/H6_{(asym)}*$ or $H6_{(asym)}''*$), 6.89 (d, $^3J_{H,H}$ = 6.1 Hz, 1H, $H6_{(asym)}*/H6_{(asym)}''*$), 6.80 (d, $^3J_{H,H}$ = 9.1 Hz, 2H, $H_{phenyl(pull)}$), 3.01 (s, 6H, $H_{methyl(NMe2)}$), 2.41 (s, 6H, $H_{methyl(SAc)}$). ^{13}C-NMR (101 MHz, CD_3CN, ppm, 22 °C): δ = 193.98 ($C_{C=O}$, 2C), 161.50 (C_q, 1C), 160.92 (C_q, 2C), 160.87 (C_q, 1C), 159.45 (C_q, 1C), 159.05 (C_q, 2C), 158.44 (C_q, 1C), 154.49 (C_t, 1C), 154.02 (C_t, 2C), 153.42 (C_q, 1C), 153.28 (C_t, 1C), 151.57 (C_q, 1C), 150.08 (C_q, 1C), 140.31 (C_q, 1C), 139.31 (C_t, 1C), 139.01 (C_t, 1C), 135.68 ($C_{phenyl(sym)}$, 4C), 134.08 (C_q, 2C), 133.48 ($C_{phenyl(sym)}$, 4C), 131.89 (C_q, 2C), 129.42 (C_t, 2C), 129.22 ($C_{phenyl(asym)}$, 2C), 129.15 ($C_{phenyl(asym)}$, 2C), 127.21 (app d, ^3J = 3.7 Hz, 2C, $C_{trifluoromethylphenyl}$), 126.28 ($C_t$, 2C), 125.89 ($C_t$, 1C), 125.14 ($C_t$, 2C), 124.91 ($C_t$, 1C), 124.76 ($C_t$, 2C), 123.60 ($C_t$, 1C), 122.92 ($C_q$, 2C), 122.84 ($C_t$, 1C), 121.83 ($C_q$, 1C), 120.74 ($C_t$, 1C), 113.15 ($C_{phenyl(asym)}$, 2C), 97.92 ($C_{acetylene}$, 2C), 87.25 ($C_{acetylene}$, 2C), 40.29 ($C_{methyl(NMe2)}$, 2C), 30.66 ($C_{methyl(SAc)}$, 2C). In the ^{13}C-spectrum two signals less than expected were found probably due to coincident signals and to the fact that the CF_3-group cannot be seen properly. ^{19}F-NMR (376 MHz, CD_3CN, ppm, 22 °C): δ = −63.36 (s, 3F, CF_3), −72.87 (d, $^1J_{P,F}$ = 706.6 Hz, 12F, PF_6). HRMS (ESI-ToF): *m/z* calcd. for $[C_{65}H_{46}F_3FeN_7O_2S_2]^{2+}$: 566.6223, found 566.6233.

5-Bromo-2-iodo-1,3-diisopropylbenzene 14: A 500 mL three-necked round bottomed flask was charged with ice (150 g) and H_2SO_4 (150 mL). 4-Bromo-2,6-diisopropylaniline (40.8 g, 15.9 mmol, 1.0 equiv.) dissolved in MeCN (80 mL) was added dropwise, while the temperature was maintained under 5 °C. Then sodium nitrite (19.8 g, 28.6 mmol, 1.8 equiv.) dissolved in ice water (80 mL) was added dropwise keeping the temperature around 0 °C. The resulting clear solution was slowly poured into a solution of potassium iodide (9.33 g, 55.7 mmol, 3.5 equiv.) dissolved in H_2O (150 mL) at room temperature and the mixture was stirred for 1 hour. The aqueous phase was extracted with DCM (3 × 30 mL) and the combined organic phases were dried over $MgSO_4$, filtered and concentrated under reduced pressure. The crude product was further purified by FCC (cyclohexane) to yield the product as light brown solid (5.19 g, 14.2 mmol, 89 %). The spectroscopic data for this compound was indentical to those reported in literature.[44]

[(4-Bromo-2,6-diisopropylphenyl)ethynyl]triisopropylsilane (15): A 250 mL round-bottomed flask was charged with 5-bromo-2-iodo-1,3-diisopropylbenzene (**14**, 2.00 g, 5.45 mmol, 1.0 equiv.), (triisopropylsilyl) acetylene (TIPSA) (1.32 mL, 5.72 mmol, 1.05 equiv.) and DIPA/toluene (1:3, 120 mL). The mixture was degassed with argon for 15 min then $Pd(dppf)Cl_2$ (99.7 mg, 136 µmol,

2.5 mol-%), and CuI (41.7 mg, 218 μmol, 4 mol-%) were added and the reaction mixture was heated to 80 °C. The reaction mixture was stirred at this temperature for two weeks. During this period several GC–MS reaction controls were performed and additional TIPSA (1.2 equiv.) was added when it was completely consumed and starting material was still left. The crude product was purified by FCC (cyclohexane) and automated GPC (chloroform) to obtain the product as slightly yellow oil (1.25 g, 2.96 mmol, 54 %).

Analytical Data for 15: ^{1}H NMR (400 MHz, CD_2Cl_2, 22 °C) δ = 7.25 (s, 2H), 3.58 (hept, J = 6.9 Hz, 2H), 1.24 (d, J = 6.9 Hz, 12H), 1.16–1.13 (m, 21H). ^{13}C NMR (101 MHz, CD_2Cl_3, 22 °C) δ = 153.94, 126.05, 123.58, 121.07, 103.07, 101.22, 32.38, 23.32, 19.00, 18.88, 12.02. HRMS (EI): calcd. for $[C_{23}H_{37}BrSi]^+$ 420.18424, found 420.18440.

{[4-(*tert*-Butylthio)-2,6-diisopropylphenyl]ethynyl}triisopropylsilane (16): A two-necked round bottomed flask was charged with 1-methyl-2-pyrrolidone (100 mL), [(4-bromo-2,6-diisopropylphenyl)ethynyl]triisopropylsilane (**15**, 2.68 g, 6.36 mmol, 1.0 equiv.), potassium carbonate (1.32 g, 9.54 mmol, 1.5 equiv.), palladium(II)-acetate (71.4 mg, 318 mmol, 5 mol-%) and 1,4-bis(diphenylphosphino)butane (138 mg, 318 mmol, 5 mol-%). The reaction mixture was degassed with argon for 15 minutes before 2-methyl-2-propane-thiol (905 mL, 7.95 mmol, 1.25 equiv.) was added and the reaction mixture was heated to 100 °C. The reaction was stirred at this temperature for 24 hours. The reaction mixture was diluted with ethyl acetate (40 mL), was washed with water (40 mL) to remove 1-methyl-2-pyrrolidone and was extracted with a 1:1 mixture of ethyl acetate (20 mL) and cyclohexane (20 mL). The combined organic phases were dried over $MgSO_4$, filtered and concentrated under reduced pressure. The crude product was purified by FCC (cyclohexane) and automated GPC (chloroform) to obtain the product as slightly orange oil (1.07 g, 2.49 mmol, 39 %).

Analytical Data for 16: ^{1}H NMR (400 MHz, $CDCl_3$, 22 °C) δ = 7.26 (s, 2H), 3.59 (hept, J = 6.9 Hz, 2H), 1.28 (s, 9H), 1.27 (d, J = 6.9 Hz, 12H), 1.16–1.14 (m, 21H). ^{13}C NMR (101 MHz, $CDCl_3$, 22 °C) δ = 151.35, 132.94, 131.22, 121.97, 103.26, 100.83, 46.25, 31.81, 31.78, 31.14, 23.29, 18.82, 11.62. HRMS (EI): calcd. for $[C_{27}H_{46}SSi]^+$ 430.30840, found 430.30819.

***tert*-Butyl(4-ethynyl-3,5-diisopropylphenyl)sulfane (17):** A round bottomed flask was charged with {[4-(*tert*-butylthio)-2,6-diisopropylphenyl]ethynyl}triisopropylsilane (**16**, 305 mg, 708 μmol, 1.0 equiv.) and DCM (50 mL). The reaction mixture was degassed with an argon stream, before TBAF (1 M in THF, 1.06 mL, 1.06 mmol, 1.5 equiv.) was added. The reaction mixture was stirred at room temperature for 10 minutes, before the solvent was removed under reduced pressure. The crude product was purified by a plug over Silica (cyclohexane) to obtain the product as slightly orange oil (194 mg, 707 μmol, 100 %).

Analytical Data for 17: ^{1}H NMR (600 MHz, CD_3CN, 25 °C) δ = 7.29 (s, 2H), 3.87 (s, 1H), 3.52 (hept, J = 6.9 Hz, 2H), 1.26 (s, 9H), 1.23 (d, J = 6.9 Hz, 12H). ^{13}C NMR (151 MHz, CD_3CN, 25 °C) δ = 152.51, 134.82, 132.01, 121.06, 88.37, 80.37, 46.70, 32.31, 31.30, 23.34. HRMS (EI): calcd. for $[C_{18}H_{26}S]^+$ 274.17497, found 274.17477.

4,4′′-Bis{[4-(*tert*-butylthio)-2,6-diisopropylphenyl]ethynyl}-2,2′:6′,2′′-terpyridine (18): 18 was prepared by adapting a literature reported protocol.[41] A two-necked round bottomed flask was charged with 4,4′′-dichloro-2,2′:6′,2′′-terpyridine (**9**, 40.0 mg, 132 μmol, 1.0 equiv.), *tert*-butyl(4-ethynyl-3,5-diisopropylphenyl)-sulfane (**17**, 93.3 mg, 340 μmol, 2.6 equiv.), Cs_2CO_3 (261 mg, 792 μmol, 6.0 equiv.), $Pd(MeCN)_2Cl_2$ (1.04 mg, 3.96 μmol, 3 mol-%) and X-Phos (5.78 mg, 11.9 μmol, 9 mol-%). The reaction flask was set under argon atmosphere before degassed propionitrile (15 mL) was added. The reaction mixture was further degassed with argon before it was heated to reflux. The reaction mixture was stirred at this temperature for 16 hours. The crude was purified by FCC (cyclohexane/ethyl acetate = 5:1 + 1 % NH_4OH) and automated GPC (chloroform) to obtain the product as white-greyish solid (67.0 mg, 86.0 μmol, 65 %).

Analytical Data for 18: ^{1}H NMR (500 MHz, $CDCl_3$, 25 °C) δ = 8.72 (dd, J = 5.0, 0.9 Hz, 2H), 8.66 (dd, J = 1.6, 0.8 Hz, 2H), 8.50 (d, J = 7.8 Hz, 2H), 8.02 (t, J = 7.8 Hz, 1H), 7.44 (dd, J = 5.0, 1.6 Hz, 2H), 7.27 (s, 4H), 3.54 (hept, J = 6.9 Hz, 4H), 1.30 (s, 18H), 1.25 (d, J = 6.9 Hz, 24H). ^{13}C NMR (126 MHz, $CDCl_3$, 25 °C) δ = 156.42, 155.14, 151.32, 149.32, 138.29, 134.33, 132.92, 131.44, 125.51, 122.96, 121.80, 120.35, 96.10, 91.16, 46.43, 31.96, 31.19, 23.29. HRMS (ESI-ToF): calcd. for $[C_{51}H_{59}N_3S_2 + H]^+$ 778.4223, found 778.4221.

S,S′-{[(2,2′:6′,2′′-Terpyridine)-4,4′′-diylbis(ethyne-2,1-diyl)]bis-(3,5-diisopropyl-4,1-phenylene)} diethanethioate (19): A round-bottomed flask was charged with 4,4′′-bis{[4-(*tert*-butylthio)-2,6-diisopropylphenyl]ethynyl}-2,2′:6′,2′′-terpyridine (**18**, 30.0 mg, 38.6 μmol, 1.0 equiv.), acetyl chloride (138 μL, 1.93 mmol, 50 equiv.), toluene (2 mL) and MeCN (2 mL). To the reaction mixture $Bi(OTf)_3$ (76.0 mg, 116 μmol, 3.0 equiv.) was added and the mixture was stirred at room temperature for 1 hour. Water (20 mL) was added and the aqueous phase was extracted with DCM (3 × 20 mL). The combined organic phases were dried over $MgSO_4$, filtered and concentrated under reduced pressure. The crude product was purified by FCC (cyclohexane/ethyl acetate = 5:1 + 1 % NH_4OH) and automated GPC (chloroform) to obtain the product as white-brownish solid (28.4 mg, 38.0 μmol, 92 %).

Analytical Data for 19: ^{1}H NMR (400 MHz, $CDCl_3$, 22 °C) δ = 8.72 (dd, J = 5.0, 0.9 Hz, 2H), 8.67–8.64 (m, 2H), 8.50 (d, J = 7.8 Hz, 2H), 8.01 (t, J = 7.8 Hz, 1H), 7.44 (dd, J = 5.0, 1.6 Hz, 2H), 7.17 (s, 4H), 3.54 (hept, J = 6.8 Hz, 4H), 2.44 (s, 6H), 1.25 (d, J = 6.9, 24H). ^{13}C NMR (126 MHz, $CDCl_3$, 25 °C) δ = 193.73, 156.44, 155.14, 152.10, 149.36, 138.28, 132.77, 129.38, 128.51, 125.49, 123.00, 121.80, 121.26, 96.27, 90.89, 32.16, 30.45, 23.15. HRMS (ESI-ToF): calcd. for $[C_{47}H_{47}N_3O_2S_2 + H]^+$ 750.3182, found 750.3186.

{[Fe(11)(19)]$^{2+}$[$(PF_6)^-$]$_2$} (5): In this case a statistic reaction had to be performed in which an equimolar amount of the terpyridine precursors was used. A 50 mL round-bottomed flask was charged with the S,S′-{[(2,2′:6′,2′′-terpyridine)-4,4′′-diylbis(ethyne-2,1-diyl)]-bis(3,5-diisopropyl-4,1-phenylene)} diethanethioate (**19**, 17.0 mg, 22.7 μmol, 1.0 equiv.), *N*,*N*-dimethyl-4-{4′′-[4-(trifluoromethyl)-phenyl]-(2,2′:6′,2′′-terpyridin)-4-yl}aniline (**12**, 11.3 mg, 22.7 μmol, 1.0 equiv.), $FeCl_2$ (3.60 mg, 28.4 μmol, 1.25 equiv.), MeOH (25 mL) and DCM (25 mL). The reaction mixture was stirred for 1 hour. The solvent was removed under reduced pressure. Water (20 mL) and sat. aq. NH_4PF_6 solution (10 mL) was added and the aqueous phase was extracted with DCM (3 × 30 mL). The combined organic layers were dried over $MgSO_4$, filtered and concentrated under reduced pressure. A plug over Silica (acetone → acetone/H_2O/sat. KPF_6 = 9:1:0.1) was performed. To obtain the desired heteroleptic target complex **5** the crude mixture was subjected to preparative reversed phase HPLC using a solvent gradient (MeCN + 1 % TFA/H_2O + 1 % TFA = 50:50 up to MeCN + 1 % TFA/H_2O + 1 % TFA = 95:5) at a flow rate of 30 mL/min. The product was isolated as dark purple solid (16.2 mg, 1.02 μmol, 45 %).

Analytical Data for 5: ^{1}H NMR (600 MHz, [D_6]Acetone, 25 °C): δ = 9.49 (d, $^3J_{H,H}$ = 8.08 Hz, 2H, $H3_{(asym)}$′, $H5_{(asym)}$′), 9.34 (d, $^3J_{H,H}$ = 8.09 Hz, 2H, $H3_{(sym)}$′, $H5_{(sym)}$′), 9.27 (d, $^4J_{H,H}$ = 1.94 Hz, 1H, $H3_{(asym)}$′′), 9.09 (d, $^4J_{H,H}$ = 2.05 Hz, 1H, $H3_{(asym)}$), 8.95 (m, 1H, $H4_{(asym)}$′), 8.95 (m, 2H, $H3_{(sym)}$, $H3_{(sym)}$′′), 8.91 (t, $^3J_{H,H}$ = 8.09 Hz, 1H, $H4_{(sym)}$′), 8.06

(d, $^{3}J_{H,H}$ = 8.3 Hz, 2H, $H2_{(phenyl(pull))}$), 7.88 (d, $^{3}J_{H,H}$ = 8.35 Hz, 2H, $H3_{(phenyl(pull))}$), 7.78 (d, $^{3}J_{H,H}$ = 9.13 Hz, 2H, $H2_{(phenyl(push))}$), 7.64 (dd, $^{3}J_{H,H}$ = 6.01 Hz, $^{4}J_{H,H}$ = 1.97 Hz, 1H, $H5_{(asym)}''$), 7.56 (d, $^{3}J_{H,H}$ = 6.03 Hz, 1H, $H6_{(asym)}''$), 7.52 (d, $^{3}J_{H,H}$ = 5.96 Hz, 2H, $H6_{(sym)}$, $H6_{(sym)}''$), 7.47 (dd, $^{3}J_{H,H}$ = 6.22 Hz, $^{4}J_{H,H}$ = 2.07 Hz, 1H, $H5_{(asym)}$), 7.37 (dd, $^{3}J_{H,H}$ = 5.97 Hz, $^{4}J_{H,H}$ = 1.74 Hz, 2H, $H5_{(sym)}$, $H5_{(sym)}''$), 7.27 (s, 4H, $H_{(phenyl(sym))}$), 7.25 (d, $^{3}J_{H,H}$ = 6.20 Hz, 1H, $H6_{(asym)}$), 6.81 (d, $^{3}J_{H,H}$ = 9.13 Hz, 2H, $H3_{(phenyl(push))}$), 3.49 (hept, $^{3}J_{H,H}$ = 6.88 Hz, 4H, H*i*Pr),), 3.04 (s, 6H, $H_{(methyl(NMe2))}$), 2.42 (s, 6H, $H_{(methyl(SAc))}$), 1.23 (d, $^{3}J_{H,H}$ = 6.91 Hz, 24H, $H_{(methyl(iPr))}$). ^{13}C NMR (151 MHz, [D_6]Acetone, 25 °C): δ = 193.06 (C_q, 2C), 161.73 (C_q, 1C), 161.16 (C_q, 2C), 161.12 (C_q, 1C), 159.84 (C_q, 1C), 159.50 (C_q, 2C), 158.77 (C_q, 1C), 154.77 (C_t, 1C), 154.08 (C_t, 2C), 153.41 (C_t, 1C), 153.36 (C_q, 1C), 153.20 (C_q, 4C), 151.66 (C_q, 1C), 150.05 (C_q, 1C), 140.34 (C_q 1C), 139.55 (C_t, 1C), 139.15 (C_t, 1C), 134.41 (C_q, 2C), 132.40 (C_q 1C), 132.16 (C_q, 2C), 129.75 (C_t, 2C), 129.34 (C_t, 4C), 129.20 (C_t, 2C), 129.07 (C_t, 2C), 127.18 (C_t, 2C), 126.04 (C_t, 1C), 125.81 (C_t, 2C), 125.47 (C_t, 2C), 125.19 (C_t, 1C), 125.02 (C_p, 1C), 125.00 (C_t, 1C), 123.66 (C_t, 1C), 122.77 (C_t, 1C), 121.85 (C_q, 1C), 120.59 (C_t, 1C), 120.49 (C_q, 2C), 113.09 (C_t, 2C), 95.55 (C_q, 2C), 95.20 (C_q, 2C), 40.14 (C_p, 2C), 32.79 (C_t, 4C), 30.44 (C_p, 2C), 23.38 (C_p, 8C). ^{19}F NMR (600 MHz, [D_6]Acetone, 25 °C): δ = –63.37 ($^{2}J_{CF}$ = 32.4 Hz, $^{1}J_{CF}$ = 271.75 Hz, 3F, CF_3), –72.42 (d, $^{1}J_{P,F}$ = 707.9 Hz, PF_6). HRMS (ESI-ToF): calcd. for $[C_{77}H_{70}F_3FeN_7O_2S_2]^{2+}$ 650.7163, found 650.1768.

Acknowledgments

The authors thank the Swiss National Science Foundation (Grant no. 200020-178808) for financial support. Furthermore, we thank Dr. Daniel Häussinger for his support with NMR-measurements and interpretation. This work was partially funded by the FET open project QuIET (no. 767187) and a European Cooperation in Science and Technology (COST) Action (MOLSPIN CA15128). M. M. acknowledges support by the 111 project (90002-18011002).

Keywords: Terpyridine · Molecular switches · Spin crossover · Molecular electronics · Break junction

[1] G. E. Moore, *Electronics* **1965**, *38*, 114–117.
[2] A. Aviram, M. A. Ratner, *Chem. Phys. Lett.* **1974**, *29*, 277–283.
[3] H. Park, J. Park, A. K. L. Lim, E. H. Anderson, A. P. Alivisatos, P. L. McEuen, *Nature* **2000**, *407*, 57–60.
[4] J. Park, A. N. Pasupathy, J. I. Goldsmith, C. Chang, Y. Yaish, J. R. Petta, M. Rinkoski, J. P. Sethna, H. D. Abruña, P. L. McEuen, et al., *Nature* **2002**, *417*, 722–725.
[5] S. Kubatkin, A. Danilov, M. Hjort, J. Cornil, J.-L. Brédas, N. Stuhr-Hansen, P. Hedegård, T. Bjørnholm, *Nature* **2003**, *425*, 698–701.
[6] M. Elbing, R. Ochs, M. Koentopp, M. Fischer, C. von Hänisch, F. Weigend, F. Evers, H. B. Weber, M. Mayor, *Proc. Natl. Acad. Sci. USA* **2005**, *102*, 8815–8820.
[7] I. Díez-Pérez, J. Hihath, Y. Lee, L. Yu, L. Adamska, M. A. Kozhushner, I. I. Oleynik, N. Tao, *Nat. Chem.* **2009**, *1*, 635–641.
[8] W. A. Reinerth, L. Jones, T. P. Burgin, C. Zhou, C. J. Muller, M. R. Deshpande, M. A. Reed, J. M. Tour, *Nanotechnology* **1998**, *9*, 246–250.
[9] J. M. Tour, *Acc. Chem. Res.* **2000**, *33*, 791–804.
[10] A. S. Blum, J. G. Kushmerick, D. P. Long, C. H. Patterson, J. C. Yang, J. C. Henderson, Y. Yao, J. M. Tour, R. Shashidhar, B. R. Ratna, *Nat. Mater.* **2005**, *4*, 167–172.
[11] S. Y. Quek, M. Kamenetska, M. L. Steigerwald, H. J. Choi, S. G. Louie, M. S. Hybertsen, J. B. Neaton, L. Venkataraman, *Nat. Nanotechnol.* **2009**, *4*, 230–234.
[12] A. R. Pease, J. O. Jeppesen, J. F. Stoddart, Y. Luo, C. P. Collier, J. R. Heath, *Acc. Chem. Res.* **2001**, *34*, 433–444.
[13] S. J. van der Molen, P. Liljeroth, *J. Phys. Condens. Matter* **2010**, *22*, 133001.
[14] J. E. Green, J. Wook Choi, A. Boukai, Y. Bunimovich, E. Johnston-Halperin, E. Delonno, Y. Luo, B. A. Sheriff, K. Xu, Y. Shik Shin, et al., *Nature* **2007**, *445*, 414–417.
[15] J. Lee, H. Chang, S. Kim, G. S. Bang, H. Lee, *Angew. Chem. Int. Ed.* **2009**, *48*, 8501–8504; *Angew. Chem.* **2009**, *121*, 8653.
[16] K. Terada, K. Kanaizuka, V. M. Iyer, M. Sannodo, S. Saito, K. Kobayashi, M. Haga, *Angew. Chem. Int. Ed.* **2011**, *50*, 6287–6291; *Angew. Chem.* **2011**, *123*, 6411.
[17] H. Song, M. A. Reed, T. Lee, *Adv. Mater.* **2011**, *23*, 1583–1608.
[18] N. Fuentes, A. Martín-Lasanta, L. Á. de Cienfuegos, M. Ribagorda, A. Parra, J. M. Cuerva, *Nanoscale* **2011**, *3*, 4003–4014.
[19] S. Lara-Avila, A. V. Danilov, S. E. Kubatkin, S. L. Broman, C. R. Parker, M. B. Nielsen, *J. Phys. Chem. C* **2011**, *115*, 18372–18377.
[20] S. T. Olsen, T. Hansen, M. B. Nielsen, M. A. Ratner, K. V. Mikkelsen, *J. Phys. Chem. C* **2017**, *121*, 3163–3170.
[21] Y. Kim, H. Song, F. Strigl, H.-F. Pernau, T. Lee, E. Scheer, *Phys. Rev. Lett.* **2011**, *106*, 196804.
[22] R. Frisenda, G. D. Harzmann, J. A. Celis Gil, J. M. Thijssen, M. Mayor, H. S. J. van der Zant, *Nano Lett.* **2016**, *16*, 4733–4737.
[23] Y.-H. Kim, H. S. Kim, J. Lee, M. Tsutsui, T. Kawai, *J. Am. Chem. Soc.* **2017**, *139*, 8286–8294.
[24] C. Bruot, J. Hihath, N. Tao, *Nat. Nanotechnol.* **2012**, *7*, 35–40.
[25] N. Darwish, I. Díez-Pérez, S. Guo, N. Tao, J. J. Gooding, M. N. Paddon-Row, *J. Phys. Chem. C* **2012**, *116*, 21093–21097.
[26] M. Baghernejad, X. Zhao, K. Baruël Ørnsø, M. Füeg, P. Moreno-García, A. V. Rudnev, V. Kaliginedi, S. Vesztergom, C. Huang, W. Hong, et al., *J. Am. Chem. Soc.* **2014**, *136*, 17922–17925.
[27] X. H. Qiu, G. V. Nazin, W. Ho, *Phys. Rev. Lett.* **2004**, *93*, 196806.
[28] B.-Y. Choi, S.-J. Kahng, S. Kim, H. Kim, H. W. Kim, Y. J. Song, J. Ihm, Y. Kuk, *Phys. Rev. Lett.* **2006**, *96*, 156106.
[29] P. Liljeroth, J. Repp, G. Meyer, *Science* **2007**, *317*, 1203–1206.
[30] L. Le Pleux, E. Kapatsina, J. Hildesheim, D. Häussinger, M. Mayor, *Eur. J. Org. Chem.* **2017**, *2017*, 3165–3178.
[31] M. Valášek, K. Edelmann, L. Gerhard, O. Fuhr, M. Lukas, M. Mayor, *J. Org. Chem.* **2014**, *79*, 7342–7357.
[32] L. Gerhard, K. Edelmann, J. Homberg, M. Valášek, S. G. Bahoosh, M. Lukas, F. Pauly, M. Mayor, W. Wulfhekel, *Nat. Commun.* **2017**, *8*, 14672.
[33] G. D. Harzmann, R. Frisenda, H. S. J. van der Zant, M. Mayor, *Angew. Chem. Int. Ed.* **2015**, *54*, 13425–13430; *Angew. Chem.* **2015**, *127*, 13624.
[34] T. Knaak, C. Gonzalez, Y. J. Dappe, G. D. Harzmann, T. Brandl, M. Mayor, R. Berndt, M. Gruber, *J. Phys. Chem. C* **2019**, *123*, 4178–4185.
[35] C. E. Housecroft, A. G. Sharpe in *Inorganic Chemistry*, *Ed. 5*, Pearson Education Limited, Harlow, **2018**, pp. 689–696.
[36] D. Aravena, E. Ruiz, *J. Am. Chem. Soc.* **2012**, *134*, 777–779.
[37] T. Miyamachi, M. Gruber, V. Davesne, M. Bowen, S. Boukari, L. Joly, F. Scheurer, G. Rogez, T. K. Yamada, P. Ohresser, et al., *Nat. Commun.* **2012**, *3*, 938.
[38] G. D. Harzmann, M. Neuburger, M. Mayor, *Eur. J. Inorg. Chem.* **2013**, *2013*, 3334–3347.
[39] G. R. Newkome, J. M. Roper, *J. Organomet. Chem.* **1980**, *186*, 147–153.
[40] C. J. Yu, Y. Chong, J. F. Kayyem, M. Gozin, *J. Org. Chem.* **1999**, *64*, 2070–2079.
[41] D. Gelman, S. L. Buchwald, *Angew. Chem. Int. Ed.* **2003**, *42*, 5993–5996; *Angew. Chem.* **2003**, *115*, 6175.
[42] E. R. T. Tiekink, J. Zukerman-Schpector, *CrystEngComm* **2009**, *11*, 1176–1186.
[43] N. Crivillers, E. Orgiu, F. Reinders, M. Mayor, P. Samorì, *Adv. Mater.* **2011**, *23*, 1447–1452.
[44] S. Sasaki, K. Kato, M. Yoshifuji, *Bull. Chem. Soc. Jpn.* **2007**, *80*, 1791–1798.

Received: March 21, 2019